Sphingomyelin upregulation in mature neurons contributes to TrkB activity by Rac1 endocytosis

Laura Trovò[1], Paul P. Van Veldhoven[2], Mauricio G. Martín[1,*] and Carlos G. Dotti[1,*]

[1]VIB, Department of Developmental Molecular Genetics and K.U.Leuven Department of Human Genetics, Herestraat 49, 3000 Leuven, Belgium
[2]K.U.Leuven, Department of Molecular Cell Biology, LIPIT, Herestraat 49, 3000 Leuven, Belgium
*Authors for correspondence (mauricio.martin@med.kuleuven.be; carlos.dotti@med.kuleuven.be)

Accepted 6 December 2010
Journal of Cell Science 124, 1308-1315

doi:10.1242/jcs.078766

Summary

A developmentally regulated loss of membrane cholesterol was reported to be sufficient and necessary for activation of neurotrophic tyrosine kinase receptor type 2 (TrkB) in aged neurons in vitro. However, TrkB activity in low cholesterol neurons remains confined to detergent-resistant membrane fractions, indicating that additional lipidic changes occur with age. Analysis of neuronal lipids at different developmental stages revealed a sharp increase in sphingomyelin (SM) during neuronal maturation. Reduction of SM abrogated TrkB activation in mature neurons, whereas increasing SM in immature neurons triggered receptor activation. TrkB activity in high SM background was the consequence of enhanced phosphorylation in the detergent-resistant fractions and increased Rac1-mediated endocytosis. The current results reveal developmental upregulation of SM as an important mechanism for sustaining TrkB activity in the mature nervous system, in addition to the presence of brain-derived neurotrophic factor (BDNF).

Key words: DRMs, Endocytosis, Rac1, Sphingomyelin, TrkB

Introduction

For neurons, the acquisition of the terminally differentiated stage implies the appearance of the full capacity to receive, process and transmit electrical information. A direct consequence of function is however the appearance of metabolic stress, due to the higher production and accumulation of reactive oxygen species from the increased need for ATP, triggered by function. Despite the presence of stress, neurons live for as long as the individual does, implying that brain cells are equipped with robust survival mechanisms.

The strength of a number of intracellular signaling events, including survival, relies on the clustering of receptors in highly ordered and dynamic lipid-based platforms (rafts) on the plasma membrane. The concept of raft has significantly changed in the last 10 years (Simons and Toomre, 2000; Simons and Gerl, 2010). At first, a protein was considered to be part of rafts as long as it was enriched in detergent-resistant membrane fractions and was sensitive to changes in cholesterol levels. The current view is far more strict, involving protein–lipid interactions that regulate the nanoscale raft protein assembly and their coalescence into larger signaling functional platforms. The presence of a protein in a detergent-resistant fraction is now taken as indication of biochemical affinity for a certain lipidic environment; a crucial issue for cell function is how membrane proteins can alter the lipid organization of the membrane by binding specific lipids and also by modifying their lipid surroundings (Niemelä et al., 2010). Interestingly, all tyrosine kinase signaling receptors, the associated adaptors, scaffolds and enzymes have high affinity for cholesterol-rich membrane fractions, as shown by their concentration into detergent-resistant fractions in response to the presence of cognate ligands (Paratcha and Ibanez, 2002; Pereira and Chao, 2007; Suzuki et al., 2004). Although it has been conclusively demonstrated that this biochemical property requires the presence of ligands, alternative mechanisms must also exist because receptor activity is found in detergent-resistant fractions even in conditions of ligand downregulation. In fact, high neurotrophic tyrosine kinase receptor type 2 (TrkB) activity was observed in the hippocampus and hippocampal neurons in vitro of brain-derived neurotrophic factor (BDNF) knockout mice and also in the hippocampus of aged wild-type mice, which have reduced BDNF levels (Martin et al., 2008). Given that this type of receptor signals upon dimerization, it became clear that one way by which activation could occur in conditions of low ligand concentration would be through changes in the lipid composition of the neuronal plasma membrane, to promote higher chances of clustering and therefore favor dimerization. In agreement with this possibility, we have shown that neuronal terminal differentiation (between 10 and 15 days in vitro (DIV)] and posterior aging (between 15 and 30 DIV) is associated with a reduction in cellular cholesterol, and that this cholesterol loss is required for TrkB activity (Martin et al., 2008). Moreover, the active receptor was found in the detergent-resistant fraction even under low cholesterol conditions. These results suggest that signaling strength requires receptor clustering in detergent-resistant platforms and that membrane receptors like TrkB have strong affinity for a particular type of cholesterol-poor but lipid-rich environment. Although in principle counter-intuitive, the existence of detergent-insoluble fractions at low cholesterol concentration has been demonstrated using model membranes containing high levels of ceramide and sphingolipids (Milhiet et al., 2002; Saslowsky et al., 2002). Similar conclusion can be drawn from studies on the brush border membrane of enterocytes (Hansen et al., 2001) and in developing neurons (Ko et al., 2005). From these results an obvious question arises: what type of lipidic change occurs after terminal differentiation to assure TrkB activity into detergent-resistant fractions? One possibility is that sphingomyelin (SM), due to its long, saturated fatty acid chains, can facilitate lipid packaging (Brown and London, 2000) and therefore favor TrkB clustering. Consistent with this possibility, SM can form separate domains in supported

Journal of Cell Science

lipid layers under conditions of low cholesterol (Lawrence et al., 2003).

Results

To test whether a rise in SM levels can explain, at least in part, the existence of robust TrkB activity in the terminally differentiated brain (Martin et al., 2008), SM was measured in synaptic membranes from 1-, 4- and 20-month-old mice (1M, 4M and 20M). Fig. 1A shows that SM levels increase from 1M to 4M (1M, 15.91±6.65; 4M, 37.75±3.52 pmol SM/nmol phospholipid; $P^{1M\text{-}4M}$=0.0011; the Student's *t*-test was used for all statistical analyses) without a further increase later on. On the other hand, the amount of total phospholipids (relative to protein) did not change (1M, 742.7±14.9; 4M, 639.34±112.7 nmol phospholipid/mg protein; $P^{1M\text{-}4M}$=0.18). In agreement with the above, detergent-resistant, phase-segregated, membranes, referred to as DRMs (detergent-resistant membranes), from hippocampal membranes of 4M mice showed 15% more SM when compared to DRMs obtained from 1M mice. An additional 15% SM increase was detected by this method between 4M and 23M. Fig. 1B shows the SM:phospholipid ratio in samples obtained from 1M, 4M and 23M mice (1M, 0.95±0.043; 4M, 1.16±0.033; 23M, 1.34±0.047; $P^{1M\text{-}4M}$=0.016, $P^{4M\text{-}23M}$=0.014, $P^{1M\text{-}23M}$=0.00019).

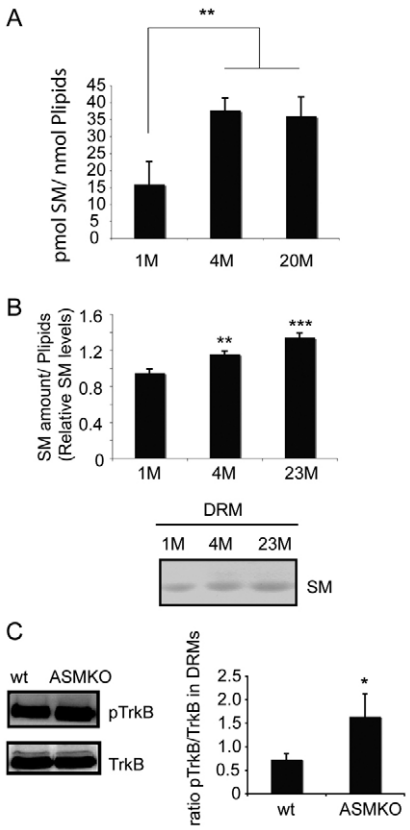

Fig. 1. Increase in SM levels during neuronal maturation in vivo. (**A**) SM levels in synaptosomes prepared from hippocampus of 1-, 4- and 20-month-old mice. SM was quantified by chromatography followed by mass analysis. Analysis reveals a 2.4-fold increase in the SM content in synaptosomes obtained from mature mice (4M) compared to young mice (1M). Values correspond to average of data obtained from four animals and are expressed in pmol SM/nmol phospholipid. (**B**) Thin layer chromatography (TLC) to determine SM levels in DRMs prepared from hippocampal membranes of 1-, 4- and 23-month-old mice. Quantification of SM bands reveals age-associated increase in the ratio of SM to phospholipids in DRMs. (**C**) Western blot showing higher levels of phospho-TrkB in DRMs of hippocampal membranes prepared from ASMKO mice compared to wild-type (wt) controls. The quantification of these experiments shows the phospho-TrKB to total TrKB ratio for each case. Bars represent mean + s.d. of at least three independent experiments. *P<0.05, **P<0.02, ***P<0.001 using Student's *t*-test.

Does the increase in SM play a role in TrkB activation in the terminally differentiated neurons? To gain insight into, this we analyzed TrkB activity in hippocampal membranes from young wild-type and acid sphingomyelinase knockout (ASMKO) mice. This is a suitable model for our purpose because the ASMKO neurons present anomalously high levels of SM at the plasma membrane with no alterations in cholesterol levels (Galvan et al., 2008) (supplementary material Fig. S1). If an increased amount of SM at the plasma membrane results in activation of TrkB receptors, then phospho-TrkB levels should be higher in the hippocampal membranes obtained from ASMKO mice compared with wild-type controls of the same age. Quantification of the western blot shown in Fig. 1C revealed higher phospho-TrkB levels (as a percentage of TrkB levels) in membranes prepared from hippocampus of ASMKO animals compared to wild-type controls (wild-type, 0.98±0.028; ASMKO, 1.5±0.25; P=0.025), thus supporting the possibility that increased SM promotes TrkB activation in neuronal cells.

To obtain more direct evidence, we used hippocampal neurons in vitro, in which SM levels can be exogenously increased or reduced. First, however, the levels of SM were measured at the different developmental stages. Lipid analysis revealed that, like the in vivo situation, hippocampal neurons in vitro undergo a developmental change in SM concentration. There was a clear increase in the SM:phospholipid ratio, which went from 32.81±5.86 pmol SM/nmol phospholipid at 10 DIV to 56.90±9.63 pmol SM/nmol phospholipids at 23 DIV (P=0.0052; Fig. 2A). To determine whether or not an SM increase occurs at the plasma membrane, fixed non-permeabilized hippocampal neurons were incubated with the SM-binding toxin lysenin, followed by anti-lysenin antibody (Fig. 2B; see Materials and Methods). The immunofluorescence images in Fig. 2B show higher plasma membrane levels in 15 DIV compared to 10 DIV neurons. Quantification of the fluorescence intensity (corrected per plasma membrane area) indicated a significant increase in SM levels between 10 DIV and 15 DIV, with no further increase between 15 DIV and 23 DIV (10 DIV, 1.00±0.19; 15 DIV, 1.65±0.30; 23 DIV, 2.01±0.25; $P^{10\text{-}15DIV}$=0.016, $P^{10\text{-}23DIV}$=0.00096, $P^{15\text{-}23DIV}$=0.09; Fig. 2B). Considering that the staining was performed in non-permeabilized neurons, the higher signal observed in old cells is most likely a reflection of plasma membrane changes.

Next, to directly assess cause and effect, the levels of the phosphorylated form of the receptor were measured in 10 DIV neurons exposed overnight to SM (the demonstration that this leads to efficient incorporation of exogenous SM is provided in supplementary material Fig. S2). Fig. 3A shows that exogenous SM addition leads to a remarkable 2.6-fold increase of phospho-TrkB in DRMs compared to control untreated cells (control, 1.00; +SM, 2.59±0.72; P=0.0354).

SM is metabolized to ceramide, and ceramide can activate the TrkA receptor in PC12 cells (MacPhee and Barker, 1999). Thus, we checked the extent to which the above effect was the direct consequence of high SM or the indirect consequence of increasing ceramide content. In favor of a direct consequence, addition of

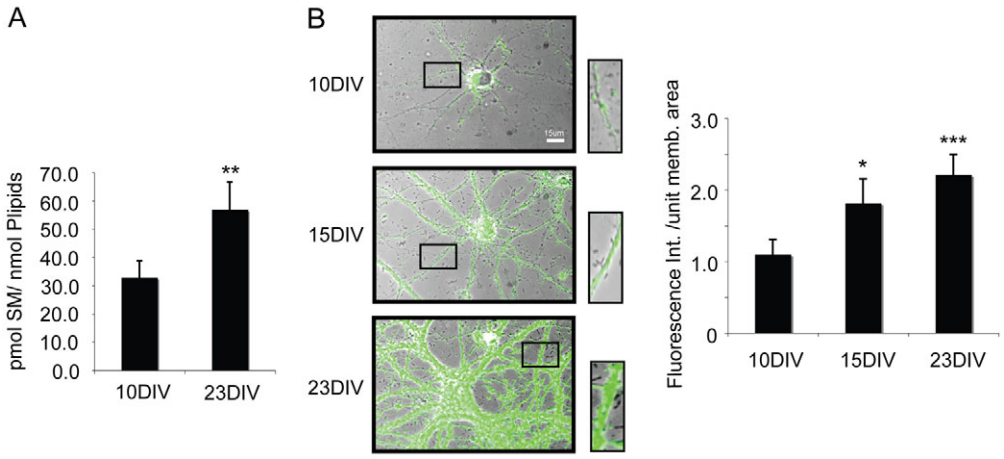

Fig. 2. Increase in SM levels after neuronal maturation in vitro. (**A**) Total SM levels measured in cell extracts by chromatography followed by mass analysis. Analysis reveals a 70% increase in the SM content obtained from aged neurons (23 DIV) compared to young neurons (10 DIV). Values correspond to average of data obtained from three different cultures and are expressed in pmol SM/nmol phospholipid. (**B**) Left panel: overlay of phase contrast and immunofluorescence microscopy images showing the increase in SM in whole neurons. SM was detected by immunofluorescence using Lysenin, and a secondary anti-Lysenin antibody. The fluorescence intensity per unit of plasma membrane, quantified in neuronal processes (as shown in the insets), is plotted on the right. Bars represent mean + s.d. of at least three independent experiments. **P*<0.05, ***P*<0.02, ****P*<0.001 compared to 10 DIV values, using Student's *t*-test.

different concentrations of ceramide to 10 DIV neurons (de Chaves et al., 2001; Stoica et al., 2005; Stoica et al., 2003; Toman et al., 2002) did not increase TrkB activation in these cells (Fig. 3B).

To further validate the idea that high SM plays a role in TrkB activity in mature neurons, we inhibited de novo synthesis of SM by the addition of Fumonisin B1 (FB1) to 14 DIV neurons, over 5 days (see Materials and Methods). Fig. 3C shows that FB1 treatment significantly lowered levels of phospho-TrkB in DRMs compared to untreated neurons of the same age (control, 1.00; FB1, 0.40±0.08; P=0.000059). Because FB1 also inhibits the generation of GM1, and GM1 can modulate TrkB activity (Pitto et al., 1998), we tested whether or not TrkB activity was reduced in old cells with low GM1 content. For this, the GM1-producing enzyme, plasma membrane ganglioside sialidase (PMGS) (Abad Rodriguez et al., 2001; Kopitz et al., 1996; Saito et al., 1995) was inhibited by the addition of NeuAc2en (2,3-dehydro-2-deoxy-*N*-acetylneuraminic acid) (Kopitz et al., 1996). This treatment did not change phospho-TrkB levels in 14 DIV neurons (supplementary material Fig. S3), indicating that the effect of FB1 corresponded to the decrease in SM. Furthermore, because a reduction in cholesterol content was shown to be sufficient to trigger TrkB activity (Martin et al., 2008), we also looked at whether SM modulation, both in gain- or loss-of-function conditions, affected TrkB phosphorylation through an indirect, cholesterol-mediated mechanism. Neither FB1 nor the addition of exogenous SM induced a significant change in cholesterol levels relative to controls (Fig. 3D).

After receptor phosphorylation, neuronal survival requires the long-lasting activation of signaling, anti-apoptotic, intermediaries. In the case of the TrkB pathway, this is guaranteed via the activation of the phosphoinositide 3-kinase (PI3K)–Akt pathway. Experiments performed in PC12 cells demonstrated that these intermediaries are activated by Trk receptors localized in signaling endosomes formed by a clathrin-independent mechanism that requires the Rho-GTPase Rac (Valdez et al., 2007). However, in cultured neurons from the central nervous system, TrkB-mediated survival signaling requires the classic clathrin–AP2 pathway (Zheng et al., 2008). These observations, and the previous demonstration that sphingolipids can influence both clathrin-dependent and independent endocytosis (Cheng et al., 2006), moved us to analyze which endocytic mechanisms contribute to the increased TrkB activity observed under high SM concentrations. First, we determined whether increased SM levels affected TrkB endocytosis.

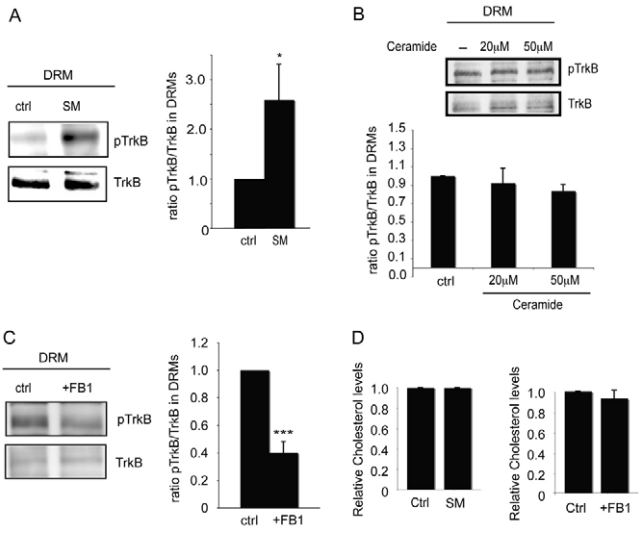

Fig. 3. SM promotes TrkB phosphorylation in DRMs. (**A**) Western blot (left panel) and its quantification (right panel) showing that SM addition to neuronal cultures results in an increased ratio of phospho-TrkB to TrkB in DRMs. (**B**) Western blot (top panel) and its quantification (bottom panel) showing that Ceramide addition to neuronal cultures does not increase TrkB phosphorylation compared to controls. (**C**) Western blot (left panel) and its quantification (right panel) showing that inhibition of SM synthesis by treatment with FB1 results in reduced TrkB activity in DRMs. (**D**) Graphs show that the treatments used to reduce or increase SM levels (see A and B) do not affect the amount of membrane cholesterol. Bars represent mean + s.d. of at least three independent experiments. **P*<0.05, ****P*<0.001 compared to control values, using Student's *t*-test.

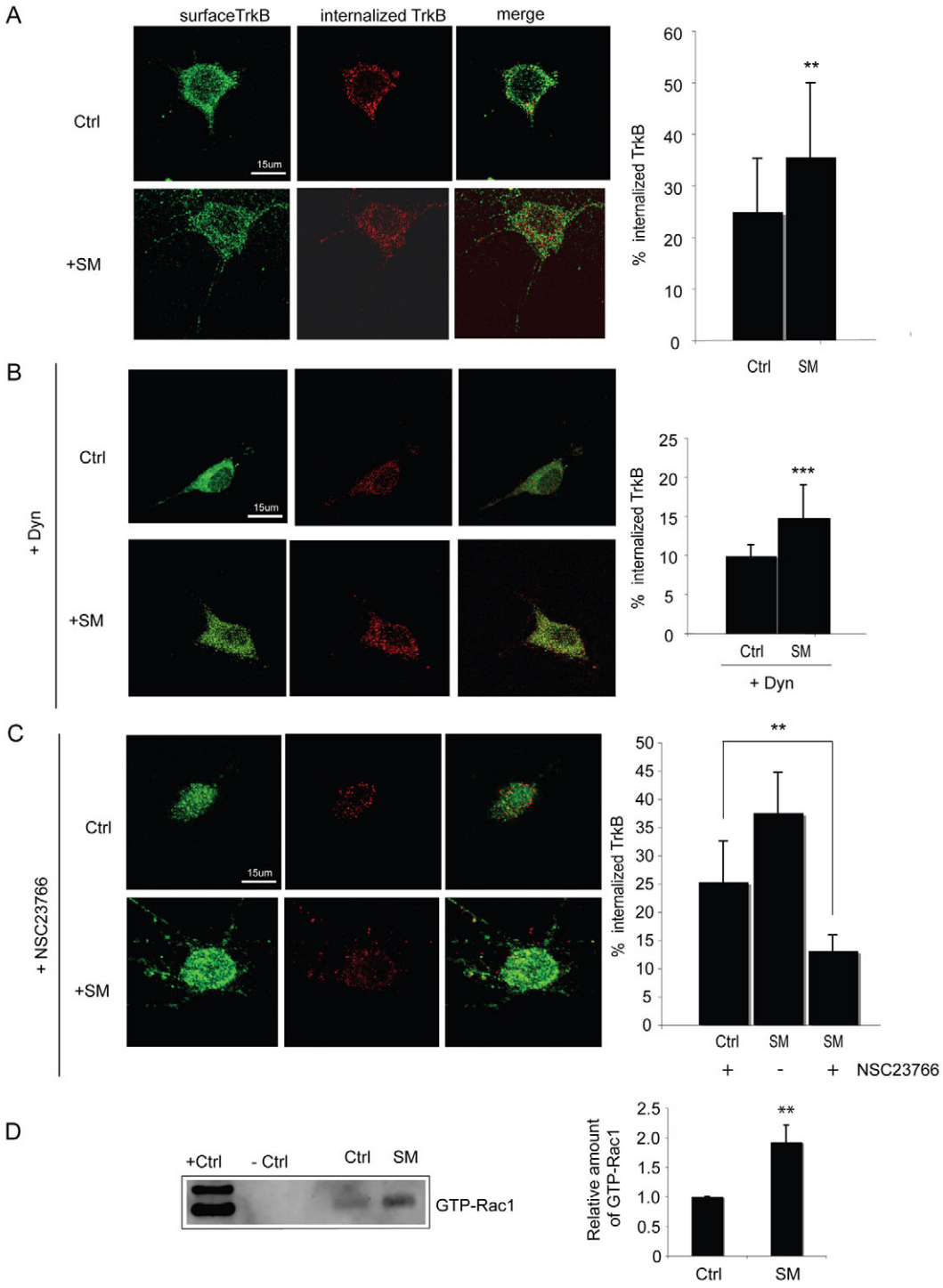

Fig. 4. SM triggers TrkB endocytosis by a Rac1-dependent mechanism in hippocampal neurons. (**A**) Left panel: Immunofluorescence performed in non-permeant and permeant conditions showing the levels of surface and internalized TrkB, respectively. TrkB was analyzed either in control (Ctrl) or in SM treated hippocampal neurons (+SM). The plot on the right shows that the percentage of internalized TrkB, obtained by quantification of the immunofluorescence images, increases after SM treatment. (**B**) Immunofluorescence images showing the levels of surface and internalized TrkB in hippocampal neurons after the blockage of dynamin-mediated endocytosis with Dynasore (+Dyn) inhibitor. Right panel: quantification of images indicates that SM increase TrkB endocytosis by a dynamin-independent mechanism. Even after Dynasore treatment, the internalized pool of TrkB is 50% higher in SM-treated cells than in controls. (**C**) Immunofluorescence images showing the levels of surface and internalized TrkB in hippocampal neurons after Rac1 inhibition with the specific inhibitor NSC23766. Right panel: quantification of images indicates that SM is not able to promote TrkB endocytosis when Rac1 is inhibited. (**D**) Western blot showing that SM treatment of young neurons results in increased levels of active GTP-Rac compared to untreated control cells (Ctrl). +Ctrl, cell lysate positive control; –Ctrl, 1 mM GDP solution negative control. Bars represent mean + s.d. of at least three independent experiments. $^{**}P<0.02$, $^{***}P<0.001$ compared to control values, using Student's *t*-test.

For this, neurons were incubated with SM followed by the immunodetection of surface and internalized TrkB (see Materials and Methods). As shown in Fig. 4A, SM treatment significantly increased the percentage of internalized TrkB (control, 25.4+10.6%; +SM, 35.5±14.4%; P=0.0028) indicating that SM is able to stimulate TrkB endocytosis.

To determine the mechanism by which SM increases TrkB endocytosis, neurons were treated either with the dynamin-inhibitor Dynasore, to block dynamin-requiring endocytic pathways, among them the clathrin-dependent pathway (Kirchhausen et al., 2008; Macia et al., 2006) or, with the Rac1-specific inhibitor NSC23766 after the addition of SM. Quantification of the ratio of surface TrkB to internalized TrkB revealed that SM-triggered TrkB internalization is not affected by dynamin inhibition (control + Dynasore, 10.0±1.0%; SM + Dynasore, 15.0±4.0%; P=0.00094, Fig. 4B). On the other hand, internalization was significantly reduced by the Rac1 inhibition in SM-treated cells (control + NSC23766, 25.4±7.2%; SM + NSC23766, 13.2±2.7%; P=0.0038, Fig. 4C). From the data in Fig. 4 it is also evident that Dynasore reduced the basal levels of TrkB internalization from 25.4±10.6%

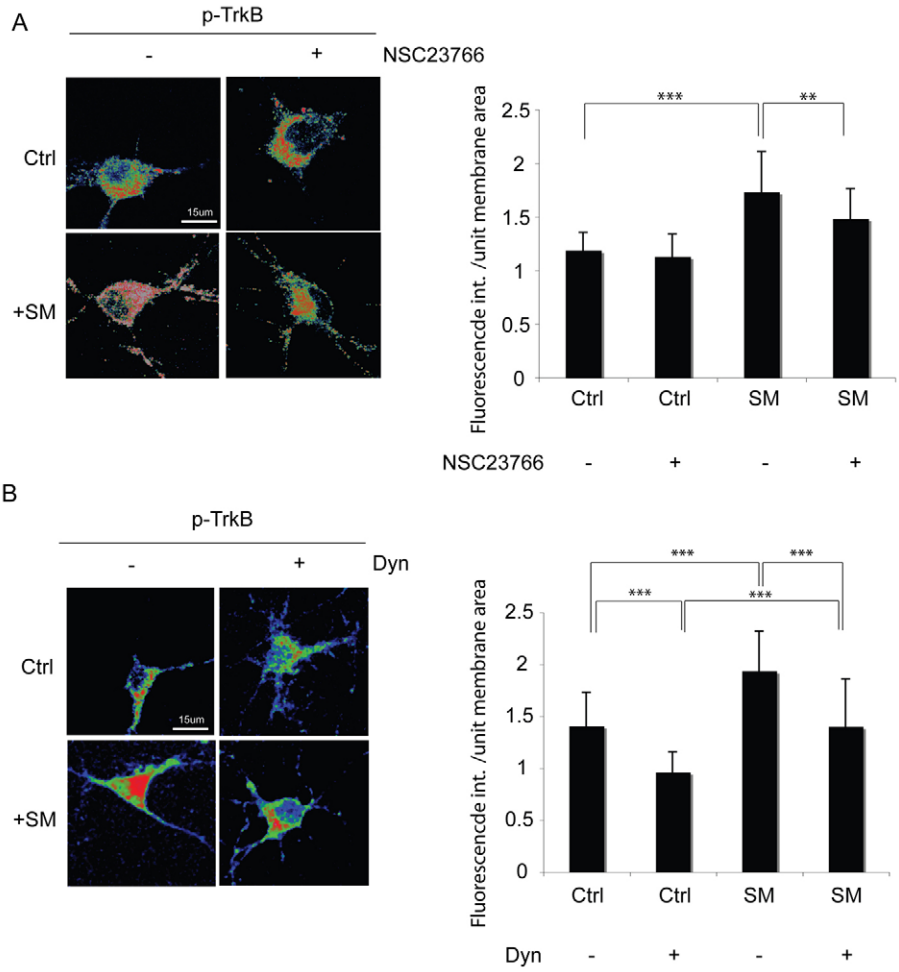

Fig. 5. SM increase is able to stimulate TrkB signaling by a Rac1-dependent pathway. (**A**) Immunofluorescence images (left) and their quantification (right) show that inhibition of Rac1-dependent endocytosis produced a significant decrease of phospho-TrkB levels in SM-treated cells, but not in control (Ctrl) neurons. (**B**) Immunofluorescence images (left) and their quantification (right) show that SM addition to neuronal cells promotes TrkB activity either in the presence or absence of Dynasore. Bars represent mean ± s.d. of at least three independent experiments. $^{**}P<0.02$, $^{***}P<0.001$ using Student's *t*-test.

to 10±1.0%; $P=1.077\times10^{-6}$) whereas NSC23766 did not affect the basal internalization rate (control + NSC23766, 25.3±7.19%; $P=0.995$). These results indicate that in control cells TrkB is mainly internalized by a dynamin-dependent mechanism and show that SM further stimulates TrkB receptor endocytosis via the activation of the Rac1-dependent (dynamin-independent) pathway. To corroborate this, we compared the levels of active Rac1 between control and SM-treated neurons. Fig. 4D shows a 1.92-fold increase in the relative level of active Rac1 in cell extracts prepared from SM-treated neurons compared to non-treated controls (control, 1.00; SM, 1.93±0.28; $P=0.0048$). Together, these results highlight the importance of Rac1 activation for total TrkB endocytosis, as a minimum under high SM conditions. It is interesting to note that the situation in hippocampal neurons is different from that observed for TrkA endocytosis in PC12 cells, in which TrkA is endocytosed by a clathrin-independent but dynamin- and Rac1-dependent mechanism (Valdez et al., 2007). The discrepancy possibly reflects differences in the basic biology between these two cell types.

Next, we analyzed the contribution of SM-triggered endocytosis on receptor activity. Control and SM-treated hippocampal neurons in culture were incubated with the Rac inhibitor NSC23766, and the levels of phosho-TrkB detected by immunofluorescence microscopy. Fig. 5A shows that Rac1 inhibitor did not affect the basal levels of TrkB activity found in untreated (control) cells (control, 1.19±0.16; control + NSC23766, 1.13±0.2; $P=0.268$) yet it reduced the higher levels of phospho-TrkB when cells were treated with SM (SM, 1.73±0.37; SM + NSC23766, 1.48±0.28; $P=0.011$).

To determine the relevance of dynamin-dependent endocytosis in receptor activity, neurons were incubated with Dynasore after SM addition. Fig. 5B shows that dynamin blockage induces a similar, 32% and 28% decrease in TrkB activity in control (control, 1.40±0.32; control + Dynasore, 0.95±0.19; $P=0.00014$) and high SM (SM, 1.93±0.38; SM + Dynasore, 1.4±0.46; $P=0.004$) samples, respectively. Together, the last series of results suggest that high SM increases TrkB activity by stimulating the Rac1-mediated process, without interfering with the dynamin-mediated process.

Because the Rac inhibitor NSC23766 strongly inhibits receptor internalization (see Fig. 4C), the fact that 31% higher TrkB phosphorylation was found in the presence of NSC23766 (Fig. 5A, compare control + NSC23766 and SM + NSC23766; $P=0.00001$) suggests that SM promotes TrkB signaling not only by turning on Rac1-dependent endocytosis but also by favoring the affinity of TrkB for DRMs (see also Fig. 3). As a matter of fact, the increase in TrkB activity after dynamin inhibition reached 47% (Fig. 5B, compare lines Ctrl+Dyn and SM+Dyn; Student's *t*-test: $P=0.0017$) due to the additional contribution of SM-triggered Rac1-mediated endocytosis. It is then likely that, in the high SM situation, a pool of receptor is activated on the neuronal surface by virtue of increasing affinity in DRMs, where they can become auto-phosphorylated. This, however, requires experimental validation with the appropriate tools.

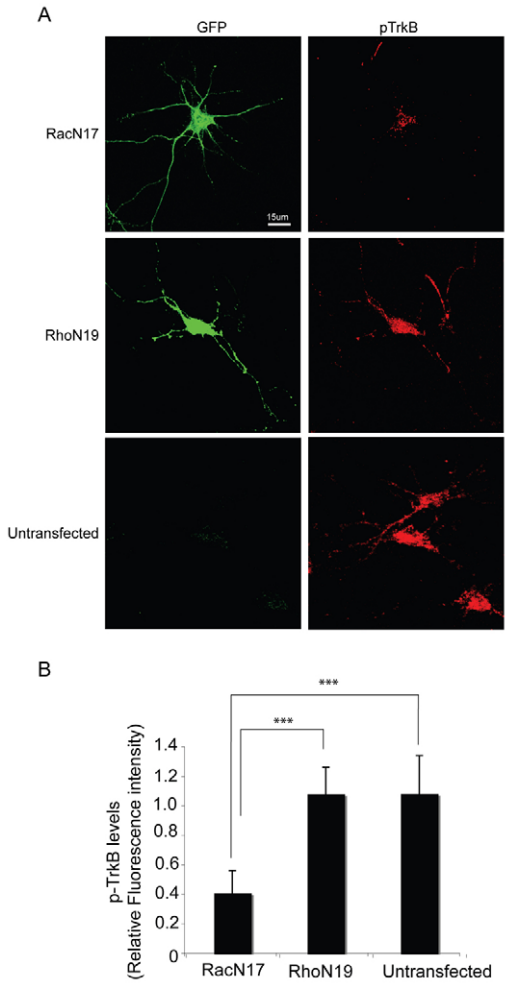

Fig. 6. Rac1 activity is required to promote TrkB phosphorylation in SM-treated neurons. (**A**) Immunofluorescence images show that SM-treated neurons overexpressing the dominant-negative form of Rac1 (RacN19), identified by GFP marker, present 62% lower levels of phospho-TrkB (red) compared to untransfected cells. No reduction in phospho-TrkB levels was observed in neurons that overexpress the dominant-negative form of RhoA (RhoN19). (**B**) Quantification of immunofluorescence images shown in A. Bars represent mean ± s.d. of at least three independent experiments. ***$P<0.001$ using Student's *t*-test.

To further demonstrate that Rac1 is required for the SM-induced TrkB internalization and signaling, the levels of phospho-TrkB were measured by immunofluorescence in SM-treated neurons transfected with RacN17, the dominant-negative mutant of Rac1. As controls, RhoN19 (the dominant-negative form of RhoA) and untransfected neurons were analyzed in this experiment. As shown in Fig. 6, RacN17 overexpression resulted in 62% decreased levels of phospho-TrkB when compared to RhoN19 or to untransfected neurons and no effect was observed when RhoN19 was used (RacN17, 0.404±0.15; untransfected, 1.048±0.25; RhoN19, 1.067±0.18; $P^{\text{RacN17-untransfected}}=5.480\times10^{-7}$; $P^{\text{RacN17-RhoN19}}=2.298\times10^{-5}$). A similar lack of effect was observed in cells treated with the cell-permeable RhoA inhibitor C3-Trans (data not shown).

Together, our results suggest that the maturation-triggered SM increase plays a role in TrkB activation through two different mechanisms: first, increased receptor affinity for particular membrane domains where it can be more efficiently phosphorylated, even independently from the presence of ligand, and second, activation of a Rac1-dependent (dynamin-independent) endocytic pathway to work in concert with the normal, dynamin-dependent, process.

Discussion

Cholesterol loss is a survival mechanism turned on by stress conditions resulting in, among other consequences, increased TrkB signaling (Martin et al., 2009). Because TrkB signaling robustness involves receptor clustering within DRMs, (Suzuki et al., 2004; Pereira and Chao, 2007; Assaife-Lopes et al., 2010) we tested the hypothesis that clustering in cells with low cholesterol neurons was provided by a compensatory rise in SM, an essential lipid, to confer detergent insolubility to membranes. In agreement with the prediction we showed, first, that neuronal terminal differentiation is accompanied by an increase in the levels of SM; second, that addition of SM to young neurons triggered the activation of TrkB; and third, that inhibition of SM synthesis in mature cells reduced the levels of active TrkB. That this mechanism is operative in vivo is suggested from experiments performed in mice lacking the gene encoding acid sphingomyelinase. These mice present high levels of SM at an early stage, and TrkB activity is higher than in wild-type counterparts (Galvan et al., 2008). Considering that, in all our experiments, increases in SM did not lead to a concomitant decrease in cholesterol levels (Fig. 3E and supplementary material Fig. S1), the evidence suggests that the increase in the ratio of SM to cholesterol (which normally occurs during maturation and aging) is an important factor in promotion of TrkB phosphorylation. This ratio-based mechanism could explain why addition of cholesterol to mature neurons reduces TrkB activity (Martin et al., 2008).

The above supposition appears contrary to the established concept that cholesterol and SM levels are coordinately regulated to maintain a constant ratio (Gupta and Rudney, 1991; Scheek et al., 1997; Slotte and Bierman, 1988; Slotte et al., 1989). This mechanism does not seem to be operative during neuronal maturation, as demonstrated by the fact that as these cells mature and age, the ratio of SM to cholesterol is changed. The reason for this might lie in the way that neurons control cholesterol and lipid metabolism. In fact, during terminal differentiation the transcription of the *cyp46A1* gene responsible for cholesterol loss is increased (Martin et al., 2008). Also, others have demonstrated the upregulation of the *cyp46* gene by reactive oxygen species, which certainly accumulate once synaptic activity is established and also over time in neurons (Martin et al., 2009; Sodero et al., 2010). It is possible that different factors that accumulate during neuronal activity (e.g. reactive oxygen species and by-products of oxidative metabolism) could trigger cholesterol elimination and SM synthesis, resulting in an increased SM to cholesterol ratio. Whether this is a general mechanism that could be applied to all types of fully differentiated cells (whether in quiescence or senescence) or if it is essential only for neurons or even neuronal subpopulations is a matter that requires further investigation. In any event, this study demonstrates the existence of a pathway that assures TrkB activity under stressful situations, which could be used in parallel to BDNF. This pathway apparently operates through the increase in the levels of SM in the plasma membrane and, by virtue of this, in the activation of an extra-internalization pathway for this receptor. In fact, TrkB is internalized by a dynamin-mediated process under steady-state levels and also by a Rac1-mediated process when the

levels of SM increase. In addition, our data suggest that high plasma membrane SM causes an increase, by a mechanism still to be defined, in the amount of active receptor at the surface. The increased internalization of TrkB under high SM conditions reported here might not be relevant for other proteins. Previous work has shown that GPI-anchored proteins are more poorly endocytosed under conditions of high neuronal SM (Galvan et al., 2008). It is possible that the differences are protein-specific and that those with natural preference to partition in DRMs (like GPI-anchored proteins) are more strongly retained by the excess of this lipid. All in all, our work defines how a lipidic change accompanying neuronal aging might contribute to an increase in the signaling strength of an essential neurotrophin receptor.

Materials and Methods

Cell culture and reagents

Primary cultures of rat embryo hippocampal neurons were prepared as previously described (Kaech and Banker, 2006). For biochemical analysis, 10^5 cells were plated into 3-cm plastic dishes coated with poly-L-lysine (0.1 mg/ml) and containing minimal essential medium with N2 supplements (MEM-N2). Neurons were kept under 5% CO_2 at 37°C.

Mice

A breeding colony of ASM heterozygous C57BL/6 mice (Horinouchi et al., 1995), kindly donated by Edward H. Schuchman (Mount Sinai School of Medicine, New York, NY), was established. The experiments were performed by comparing littermates of wild-type or ASMKO mice (4 months of age); the genotype was determined from genomic DNA in a PCR reaction.

Cell treatments and transfections

To decrease membrane sphingolipids, Fumonisin B1 (Sigma-Aldrich) was added at a final concentration of 25 μM every 48 hours over 5 days, starting from 14 DIV neurons (Harel and Futerman, 1993; Ledesma et al., 1999; Ledesma et al., 1998). SM (bovine brain, ≥97.0%; Sigma-Aldrich) was dissolved in ethanol (50 mM stock solution) and added to the neuronal medium at a final concentration of 50 μM. Cells were incubated overnight at 37°C (Ledesma et al., 1998). Non-hydroxy fatty acid ceramide from bovine brain (Sigma-Aldrich) was dissolved in choloform (10 mg/ml stock solution) and added to the medium at a final concentration of 20 μM or 50 μM. Cells were incubated overnight at 37°C (de Chaves et al., 2001; Stoica et al., 2005; Stoica et al., 2003; Toman et al., 2002).

Plasmids expressing the dominant-negative forms of small GTPases were obtained by cloning of either N17 Rac or N17 cdc fragments (Ridley et al., 1992) into pEGFP-C3 vector (Clontech) via *Eco*RI/*Sal*I restriction sites. For transfection, a calcium phosphate precipitation protocol was used (Kohrmann et al., 1999). Neurons grown on 15-mm coverslips were transferred to 3.5-cm dishes containing 2 ml of conditioned medium. Plasmid DNA (3 μg) was dissolved in 60 μl of 250 mM $CaCl_2$. A 2× concentration of BBS (280 mM NaCl, 1.5 mM Na_2HPO_4, and 50 mM *N*,*N*-bis[2-hydroxyethyl]-2-aminoethanesulfonic acid, pH 7.05) was added slowly, and the precipitate was allowed to form for 5 minutes. This solution was added to the cells, and the dishes were incubated for 1–2 hours at 37°C and 2.5% CO_2. Cells were then washed twice in HBS (135 mM NaCl, 20 mM HEPES, 4 mM KCl, 1 mM Na_2HPO_4, 2 mM $CaCl_2$, 1 mM $MgCl_2$, and 10 mM glucose, pH 7.05) before the original growth medium was added. Analysis of transfected cells was performed 24 hours after the transfection.

Protein extract and membrane preparation

Extracts from mice hippocampi were prepared in 25 mM MES pH 7.0, 5 mM DTT, 2 mM EDTA, protease inhibitor cocktail, 1 mM sodium orthovanadate and 1 mM sodium fluoride using a Dounce homogenizer and ten passages through a 24-gauge syringe needle. Hippocampal neurons were scraped in the same buffer and homogenized by ten passages through a 24-gauge syringe. The samples were centrifuged for 10 minutes at 1000 ***g*** and the supernatants were considered as total extracts. A further centrifugation was performed at 66,000 ***g*** for 1 hour at 4°C to pellet the membrane fraction. Protein concentration was quantified by the BCA method (Bio-Rad).

Isolation of detergent-resistant membranes

DRMs were prepared by treating either total extracts or membrane preparations with 1% Triton-X 100 in 25 mM MES pH 7.0, 5 mM DTT, 2 mM EDTA, protease inhibitor cocktail, 1 mM sodium orthovanadate and 1 mM sodium fluoride, at 4°C for 1 hour with shaking. The DRM pellet was obtained by centrifugation at 66,000 ***g*** for 1 hour at 4°C and resuspended in 1× Laemmli sample loading buffer, or used for lipid extraction.

Western blotting and antibodies

Proteins separated by PAGE were transferred to nitrocellulose membranes at 100 V for 1 hour and probed with a polyclonal rabbit anti-Trk (Cell Signaling Technology), and anti-pTrk (SantaCruz Biotechnology). Species-specific peroxidase-conjugated secondary antibodies were subsequently used to perform enhanced chemiluminescence detection (Amersham ECL Western Blotting; GE Healthcare, Little Chalfont, UK). Quantification was done by densitometry of the images using the NIH ImageJ software.

Lipid determination

Lipid extracts were prepared from synaptosomes isolated as described previously (Dunkley et al., 2008), from DRM pellets or from monolayers, the latter scraped in methanol (Van Veldhoven and Bell, 1988), as described (Bligh and Dyer, 1959). Extracts were analyzed either directly or following TLC (silica 60G; solvent chloroform/methanol/formic acid 65/25/10, v/v) for phospholipid organic phosphate (Van Veldhoven and Bell, 1988), SM organic phosphate (Van Veldhoven and Bell, 1988) or choline content.

For a qualitative SM determination, lipid extracts were subjected to a double development. Thefirst solvent was chloroform/acetone/acetic acid/methanol/water (50:20:10:10:5) to separate phospholipids and the second solvent was hexane/ethyl acetate (5:2). After drying, the plate was sprayed with 7% sulfuric acid and heated at 150°C, followed by scanning of the areas corresponding to SM. Cholesterol was measured in membrane pellets, resuspended in 1× PBS containing 0.2% SDS, using the Amplex Red Cholesterol Assay Kit (Molecular Probes).

Immunofluorescence microscopy

For cytoimmunochemical detection of SM, neurons on glass coverslips were washed twice in 1× PBS and then fixed with 4% paraformaldehyde/sucrose. After three washes in PBS, neurons were incubated with 0.1 ug/ml Lysenin (PeptaNova) in PBS overnight at 4°C in a humidified chamber. The surface distribution of SM was detected with anti-Lysenin antibody (PeptaNova) and species-specific FITC-conjugated secondary antibody.

For the fluorescence internalization assay, hippocampal neurons were labeled for 10 minutes at 37°C with an antibody directed against the extracellular region of TrkB receptor. After washes in PBS, neurons were incubated at 37°C in conditioned growth medium containing pharmacological agents for 30 minutes. Dynasore (Sigma) was added at final concentration of 80 μM and Rac inhibitor NSC23766 (Calbiochem) was added at final concentration of 200 μM as indicated (Gao et al., 2004; Rex et al., 2009). Neurons were fixed for 10 minutes with 4% paraformaldehyde/sucrose without permeabilization, and stained with species-specific FITC-conjugated secondary antibody for 1 hour at room temperature, to visualize prelabeled surface receptor. Then cells were permeabilized for 1 minute in 100% methanol at –20°C and stained with TRITC-conjugated secondary antibody for 1 hour at room temperature, to visualize prelabeled internalized receptors. The internalization rate was quantified by the ratio of red intensity (indicative of internalization) to total (red + green) fluorescence intensities using the NIH ImageJ software (Bhattacharyya et al., 2009; Lee et al., 2000).

To analyze the activity of the TrkB receptor, fixed neurons were labeled with an antibody against phospho-TrkB. Quantification was performed using the NIH ImageJ software, and signal intensity was normalized by area.

Rac1 activity assay

To determine the amount of active Rac1 in either control or SM-treated neurons, a Rac Activation Assay Kit (Cell Biolabs) was used. Active Rac1 from fresh cellular homogenates was column-purified by affinity to its downstream effector p21-binding domain of p21-activated protein kinase. Active Rac1 was eluted from the column and analyzed by western blot using anti-Rac1 antibodies provided in the kit.

We thank Kristel Vennekens and Tatiana Estrada Hernandez for technical assistance. The following institutions provided financial support: Fund for Scientific Research Flanders (FWO) G.0581.09 to P.P.V.V. and Fund for Scientific Research Flanders, Federal Office for Scientific Affairs (IUAP P6/43), SAO-FRMA Grant and Flemish Government's Methusalem Grant to C.G.D.

Supplementary material available online at
http://jcs.biologists.org/cgi/content/full/124/8/1308/DC1

References

Abad Rodriguez, J., Piddini, E., Hasegawa, T., Miyagi, T. and Dotti, C. G. (2001). Plasma membrane ganglioside sialidase regulates axonal growth and regeneration in hippocampal neurons in culture. *J. Neurosci.* **21**, 8387-8395.

Assaife-Lopes, N., Sousa, V. C., Pereira, D. B., Ribeiro, J. A., Chao, M. V. and Sebastiao, A. M. (2010). Activation of adenosine A2A receptors induces TrkB translocation and increases BDNF-mediated phospho-TrkB localization in lipid rafts: implications for neuromodulation. *J. Neurosci.* **30**, 8468-8480.

Bhattacharyya, S., Biou, V., Xu, W., Schluter, O. and Malenka, R. C. (2009). A critical role for PSD-95/AKAP interactions in endocytosis of synaptic AMPA receptors. *Nat. Neurosci.* **12**, 172-181.

Bligh, E. G. and Dyer, W. J. (1959). A rapid method of total lipid extraction and purification. *Can. J. Biochem. Physiol.* **37**, 911-917.

Brown, D. A. and London, E. (2000). Structure and function of sphingolipid- and cholesterol-rich membrane rafts. *J. Biol. Chem.* **275**, 17221-17224.

Cheng, Z. J., Singh, R. D., Sharma, D. K., Holicky, E. L., Hanada, K., Marks, D. L. and Pagano, R. E. (2006). Distinct mechanisms of clathrin-independent endocytosis have unique sphingolipid requirements. *Mol. Biol. Cell* **17**, 3197-3210.

de Chaves, E. P., Bussiere, M., MacInnis, B., Vance, D. E., Campenot, R. B. and Vance, J. E. (2001). Ceramide inhibits axonal growth and nerve growth factor uptake without compromising the viability of sympathetic neurons. *J. Biol. Chem.* **276**, 36207-36214.

Dunkley, P. R., Jarvie, P. E. and Robinson, P. J. (2008). A rapid Percoll gradient procedure for preparation of synaptosomes. *Nat. Protoc.* **3**, 1718-1728.

Galvan, C., Camoletto, P. G., Cristofani, F., Van Veldhoven, P. P. and Ledesma, M. D. (2008). Anomalous surface distribution of glycosyl phosphatidyl inositol-anchored proteins in neurons lacking acid sphingomyelinase. *Mol. Biol. Cell* **19**, 509-522.

Gao, Y., Dickerson, J. B., Guo, F., Zheng, J. and Zheng, Y. (2004). Rational design and characterization of a Rac GTPase-specific small molecule inhibitor. *Proc. Natl. Acad. Sci. USA* **101**, 7618-7623.

Gupta, A. K. and Rudney, H. (1991). Plasma membrane sphingomyelin and the regulation of HMG-CoA reductase activity and cholesterol biosynthesis in cell cultures. *J. Lipid Res.* **32**, 125-136.

Hansen, G. H., Immerdal, L., Thorsen, E., Niels-Christiansen, L. L., Nystrom, B. T., Demant, E. J. and Danielsen, E. M. (2001). Lipid rafts exist as stable cholesterol-independent microdomains in the brush border membrane of enterocytes. *J. Biol. Chem.* **276**, 32338-32344.

Harel, R. and Futerman, A. H. (1993). Inhibition of sphingolipid synthesis affects axonal outgrowth in cultured hippocampal neurons. *J. Biol. Chem.* **268**, 14476-14481.

Horinouchi, K., Erlich, S., Perl, D. P., Ferlinz, K., Bisgaier, C. L., Sandhoff, K., Desnick, R. J., Stewart, C. L. and Schuchman, E. H. (1995). Acid sphingomyelinase deficient mice: a model of types A and B Niemann-Pick disease. *Nat. Genet.* **10**, 288-293.

Kaech, S. and Banker, G. (2006). Culturing hippocampal neurons. *Nat. Protoc.* **1**, 2406-2415.

Kirchhausen, T., Macia, E. and Pelish, H. E. (2008). Use of dynasore, the small molecule inhibitor of dynamin, in the regulation of endocytosis. *Methods Enzymol.* **438**, 77-93.

Ko, M., Zou, K., Minagawa, H., Yu, W., Gong, J. S., Yanagisawa, K. and Michikawa, M. (2005). Cholesterol-mediated neurite outgrowth is differently regulated between cortical and hippocampal neurons. *J. Biol. Chem.* **280**, 42759-42765.

Kohrmann, M., Haubensak, W., Hemraj, I., Kaether, C., Lessmann, V. J. and Kiebler, M. A. (1999). Fast, convenient, and effective method to transiently transfect primary hippocampal neurons. *J. Neurosci. Res.* **58**, 831-835.

Kopitz, J., von Reitzenstein, C., Sinz, K. and Cantz, M. (1996). Selective ganglioside desialylation in the plasma membrane of human neuroblastoma cells. *Glycobiology* **6**, 367-376.

Lawrence, J. C., Saslowsky, D. E., Edwardson, J. M. and Henderson, R. M. (2003). Real-time analysis of the effects of cholesterol on lipid raft behavior using atomic force microscopy. *Biophys. J.* **84**, 1827-1832.

Ledesma, M. D., Simons, K. and Dotti, C. G. (1998). Neuronal polarity: essential role of protein-lipid complexes in axonal sorting. *Proc. Natl. Acad. Sci. USA* **95**, 3966-3971.

Ledesma, M. D., Brugger, B., Bunning, C., Wieland, F. T. and Dotti, C. G. (1999). Maturation of the axonal plasma membrane requires upregulation of sphingomyelin synthesis and formation of protein-lipid complexes. *EMBO J.* **18**, 1761-1771.

Lee, H. K., Barbarosie, M., Kameyama, K., Bear, M. F. and Huganir, R. L. (2000). Regulation of distinct AMPA receptor phosphorylation sites during bidirectional synaptic plasticity. *Nature* **405**, 955-959.

Macia, E., Ehrlich, M., Massol, R., Boucrot, E., Brunner, C. and Kirchhausen, T. (2006). Dynasore, a cell-permeable inhibitor of dynamin. *Dev. Cell* **10**, 839-850.

MacPhee, I. and Barker, P. A. (1999). Extended ceramide exposure activates the trkA receptor by increasing receptor homodimer formation. *J. Neurochem.* **72**, 1423-1430.

Martin, M. G., Perga, S., Trovo, L., Rasola, A., Holm, P., Rantamaki, T., Harkany, T., Castren, E., Chiara, F. and Dotti, C. G. (2008). Cholesterol loss enhances TrkB signaling in hippocampal neurons aging in vitro. *Mol. Biol. Cell* **19**, 2101-2112.

Martin, M. G., Trovo, L., Perga, S., Sadowska, A., Rasola, A., Chiara, F. and Dotti, C. G. (2009). Cyp46-mediated cholesterol loss promotes survival in stressed hippocampal neurons. *Neurobiol. Aging* (Epub ahead of print).

Milhiet, P. E., Giocondi, M. C. and Le Grimellec, C. (2002). Cholesterol is not crucial for the existence of microdomains in kidney brush-border membrane models. *J. Biol. Chem.* **277**, 875-878.

Niemelä, P. S., Miettinen, M. S., Monticelli, L., Hammaren, H., Bjelkmar, P., Murtola, T., Lindahl, E. and Vattulainen, I. (2010). Membrane proteins diffuse as dynamic complexes with lipids. *J. Am. Chem. Soc.* **132**, 7574-7575.

Paratcha, G. and Ibanez, C. F. (2002). Lipid rafts and the control of neurotrophic factor signaling in the nervous system: variations on a theme. *Curr. Opin. Neurobiol.* **12**, 542-549.

Pereira, D. B. and Chao, M. V. (2007). The tyrosine kinase Fyn determines the localization of TrkB receptors in lipid rafts. *J. Neurosci.* **27**, 4859-4869.

Pitto, M., Mutoh, T., Kuriyama, M., Ferraretto, A., Palestini, P. and Masserini, M. (1998). Influence of endogenous GM1 ganglioside on TrkB activity, in cultured neurons. *FEBS Lett.* **439**, 93-96.

Rex, C. S., Chen, L. Y., Sharma, A., Liu, J., Babayan, A. H., Gall, C. M. and Lynch, G. (2009). Different Rho GTPase-dependent signaling pathways initiate sequential steps in the consolidation of long-term potentiation. *J. Cell Biol.* **186**, 85-97.

Ridley, A. J., Paterson, H. F., Johnston, C. L., Diekmann, D. and Hall, A. (1992). The small GTP-binding protein rac regulates growth factor-induced membrane ruffling. *Cell* **70**, 401-410.

Saito, M., Tanaka, Y., Tang, C. P., Yu, R. K. and Ando, S. (1995). Characterization of sialidase activity in mouse synaptic plasma membranes and its age-related changes. *J. Neurosci. Res.* **40**, 401-406.

Saslowsky, D. E., Lawrence, J., Ren, X., Brown, D. A., Henderson, R. M. and Edwardson, J. M. (2002). Placental alkaline phosphatase is efficiently targeted to rafts in supported lipid bilayers. *J. Biol. Chem.* **277**, 26966-26970.

Scheek, S., Brown, M. S. and Goldstein, J. L. (1997). Sphingomyelin depletion in cultured cells blocks proteolysis of sterol regulatory element binding proteins at site 1. *Proc. Natl. Acad. Sci. USA* **94**, 11179-11183.

Simons, K. and Gerl, M. J. (2010). Revitalizing membrane rafts: new tools and insights. *Nat. Rev. Mol. Cell Biol.* **11**, 688-699.

Simons, K. and Toomre, D. (2000). Lipid rafts and signal transduction. *Nat. Rev. Mol. Cell Biol.* **1**, 31-39.

Slotte, J. P. and Bierman, E. L. (1988). Depletion of plasma-membrane sphingomyelin rapidly alters the distribution of cholesterol between plasma membranes and intracellular cholesterol pools in cultured fibroblasts. *Biochem. J.* **250**, 653-658.

Slotte, J. P., Hedstrom, G., Rannstrom, S. and Ekman, S. (1989). Effects of sphingomyelin degradation on cell cholesterol oxidizability and steady-state distribution between the cell surface and the cell interior. *Biochim. Biophys. Acta* **985**, 90-96.

Sodero, A. O., Weissmann, C., Ledesma, M. D. and Dotti, C. G. (2010). Cellular stress from excitatory neurotransmission contributes to cholesterol loss in hippocampal neurons aging in vitro. *Neurobiol. Aging* [Epub ahead of print] doi:10.1016/j.neurobiolaging.2010.06.001.

Stoica, B. A., Movsesyan, V. A., Lea, P. M. t. and Faden, A. I. (2003). Ceramide-induced neuronal apoptosis is associated with dephosphorylation of Akt, BAD, FKHR, GSK-3beta, and induction of the mitochondrial-dependent intrinsic caspase pathway. *Mol. Cell. Neurosci.* **22**, 365-382.

Stoica, B. A., Movsesyan, V. A., Knoblach, S. M. and Faden, A. I. (2005). Ceramide induces neuronal apoptosis through mitogen-activated protein kinases and causes release of multiple mitochondrial proteins. *Mol. Cell. Neurosci.* **29**, 355-371.

Suzuki, S., Numakawa, T., Shimazu, K., Koshimizu, H., Hara, T., Hatanaka, H., Mei, L., Lu, B. and Kojima, M. (2004). BDNF-induced recruitment of TrkB receptor into neuronal lipid rafts: roles in synaptic modulation. *J. Cell Biol.* **167**, 1205-1215.

Toman, R. E., Movsesyan, V., Murthy, S. K., Milstien, S., Spiegel, S. and Faden, A. I. (2002). Ceramide-induced cell death in primary neuronal cultures: upregulation of ceramide levels during neuronal apoptosis. *J. Neurosci. Res.* **68**, 323-330.

Valdez, G., Philippidou, P., Rosenbaum, J., Akmentin, W., Shao, Y. and Halegoua, S. (2007). Trk-signaling endosomes are generated by Rac-dependent macroendocytosis. *Proc. Natl. Acad. Sci. USA* **104**, 12270-12275.

Van Veldhoven, P. P. and Bell, R. M. (1988). Effect of harvesting methods, growth conditions and growth phase on diacylglycerol levels in cultured human adherent cells. *Biochim. Biophys. Acta* **959**, 185-196.

Zheng, J., Shen, W. H., Lu, T. J., Zhou, Y., Chen, Q., Wang, Z., Xiang, T., Zhu, Y. C., Zhang, C., Duan, S. et al. (2008). Clathrin-dependent endocytosis is required for TrkB-dependent Akt-mediated neuronal protection and dendritic growth. *J. Biol. Chem.* **283**, 13280-13288.